

Magneto optics of single photons emitted from single InAs/GaAs self-assembled quantum dots in a planar microcavity

S. Alon-Braitbart^a, E. Poem^a, L. Fradkin^a, N. Akopian^a, S. Vilan^a, E. Lifshitz^a,
E. Ehrenfreund^a, D. Gershoni^a, B.D. Gerardot^b, A. Badolato^b, P.M. Petroff^{b,*}

^a*Solid State Institute, Technion-Israel Institute of Technology, Haifa 32000, Israel*

^b*Materials Department, University of California, Santa Barbara, CA 93106, USA*

Abstract

We fully characterize the fine spectral structure of neutral and negatively charged single microcavity quantum dot excitons, using polarization-sensitive magneto-photoluminescence spectroscopy. We show that the microcavity allows the simultaneous detection of both the bright and dark excitons using Faraday configuration. Thus, we were able to fully determine the fine structure and the g -factors of the neutral and negatively charged single exciton states within the same single quantum dot. Our measurements are in excellent agreement with novel, many carrier model calculations, which take into account Coulomb and exchange interactions among all the confined e–h pair states.

© 2006 Published by Elsevier B.V.

PACS: 78.67.Hc; 71.35.Pq; 72.25.Fe; 71.35.Cc

Keywords: QD; Quantum dot; Exciton; Fine structure; Microcavity; g -factor; Diamagnetic shift

1. Introduction

Semiconductor quantum dots (QDs) have been extensively investigated as potential, technology-compatible quantum light emitters [1–4] providing single photons or “flying qubits” on demand. Such devices are important for possible future applications like quantum information processing and cryptography [5,6].

In this study, we use magneto optical spectroscopy of single QDs embedded in planar microcavity (PMC) in order to explore the fine spectral structure of the fundamental optical excitation of these novel quantum light sources. In particular, we study neutral and negatively charged single excitons (X^0 and X^{-1}), confined in the same single QD. The PMC [7], which was designed to resonate with the exciton emission, forces photons to propagate on the surface of an imaginary “light cone” with the QD on its apex. The cone angle depends on the detuning of the photon energy above the energy of the cavity mode. By

applying external magnetic field normal to the PMC plane or along the symmetry axis of the light cone (Faraday configuration), detuned photons propagate at an angle relative to the magnetic field direction. This makes possible the detection of otherwise “forbidden” optical transitions, conventionally termed as “dark” excitons. The ability to observe the allowed (“bright”) and dark optical transitions for both the neutral and negatively charged excitons enables us to fully characterize the fine structure of the QD exciton.

2. Theoretical model

In cylindrically symmetric QDs, the neutral exciton (X^0) can be viewed as composed of two confined charge carriers, an electron with spin projection of $\pm\frac{1}{2}$ on the QDs symmetry axis, and a heavy hole with spin projection of $\pm\frac{3}{2}$. The four-fold degeneracy of the various spin combinations is removed by the isotropic electron–hole exchange interaction (EHXI). The EHXI energetically separates the states in which the carriers spins are parallel (“dark”

*Corresponding author.

E-mail address: petroff@engineering.ucsb.edu (P.M. Petroff).

excitons, total spin projection $|\pm 2\rangle$) from the states in which they are anti-parallel (“bright” excitons $|\pm 1\rangle$). The $+1(-1)$ bright exciton radiative recombination is allowed and it may result in the emission of right (left) hand circularly polarized photon, propagating along the QD symmetry axis.

Self-assembled QDs are naturally asymmetrical and hence, the remaining degeneracy is completely removed by the anisotropic EHXI which distinguishes between the symmetric and anti-symmetric combinations of the $|\pm 1\rangle$ ($|\pm 2\rangle$) of the bright (dark) exciton states. The emitted photon in this case will be linearly polarized parallel (perpendicular) to the QD longer asymmetry axis. Typically, the isotropic EHXI (Δ_0 , few hundreds μeV) is almost an order of magnitude larger than the anisotropic EHXI (Δ_1 and Δ_2). When a strong magnetic field is applied along the symmetry axis of the QD (Faraday configuration), the Zeeman energy largely exceeds the anisotropic EHXI, the cylindrical symmetry is effectively restored, the energy of the four different spin configurations is determined by the spin alignment of the carriers and the emitted photons are circularly polarized (see inset to Fig. 3a) [8–10].

The magnetic field directly influences the charge carriers as described by the Hamiltonian [10] $H_B = e^2 / (8m_{e(h)\parallel} c^2) r_{e(h)}^2 B^2$, where e is the electric charge, c the speed of light, B is the magnetic field magnitude, $m_{e(h)\parallel}$ is the electron (hole) inplane effective mass and $r_{e(h)}$ is its position operator. This Hamiltonian results in a diamagnetic shift in the excitonic transition energies, with a proportionality constant, which depends on the exciton spatial extent [10].

Negatively charged exciton (or trion) involves three charge carriers: two electrons with opposite spins in the ground state of the conduction band, and one hole in the ground valence band. Since the net electronic spin is zero, there is no EHXI and in the absence of magnetic field, the two $\pm \frac{3}{2}$ spin states $|(\uparrow\downarrow)\uparrow\rangle$ and $|(\uparrow\downarrow)\downarrow\rangle$ are (Kramer’s) degenerate. Optical recombination results in singly charged two final $\pm \frac{1}{2}$ electron spin states $|\uparrow\rangle$ and $|\downarrow\rangle$, respectively, which are also degenerate. Thus, four degenerate transitions are possible between the initial trion states and the

final electronic states. Two are optically allowed and result in circularly polarized photons and two are forbidden. In the presence of magnetic field, the degeneracy of the initial trion state is removed by the hole’s Zeeman energy and the degeneracy of the final state is removed by the electron’s Zeeman energy. The effective Zeeman splitting of the X^{-1} transition is therefore identical to that of the X^0 in strong fields.

3. Experiment and discussion

We used PMC [13] embedded QDs samples. The samples were grown by molecular beam epitaxy on a (100)-oriented GaAs substrate. One layer of strain-induced InAs QDs was deposited in the center of a one wavelength GaAs PMC formed by two unequal stacks of alternating quarter wavelength layers of AlAs and GaAs, respectively. The height of the QDs was controlled by partially covering the InAs QDs with a 3 nm layer of GaAs and subsequent growth interruption. The PMC was designed to have a relatively low Q factor (200) and a cavity length, which matches the wavelength of the QD emission due to ground level e–h pair recombination. The samples were not patterned or processed laterally to prevent obscuration of the emission polarization.

A diffraction-limited, scanning confocal optical microscope was used for the photoluminescence (PL) studies of these single PMC QDs [11,12]. The microscope was inserted into the bore of a superconducting magnet such that the measurements were performed at liquid helium temperature (4.2 K) and axial magnetic fields of up to 10 T. For excitation, we used a cw laser in the wavelength range of 700 nm. A 0.75 m monochromator followed by a liquid nitrogen cooled CCD detector were used for monitoring the PL. We obtained spectral resolution of 20 μeV . The polarization state of the emitted light was monitored by the use of liquid crystal variable retarders and high-quality polarizers.

The PL spectrum of a single, resonant PMC QD comprises of a few spectral lines, depending on the

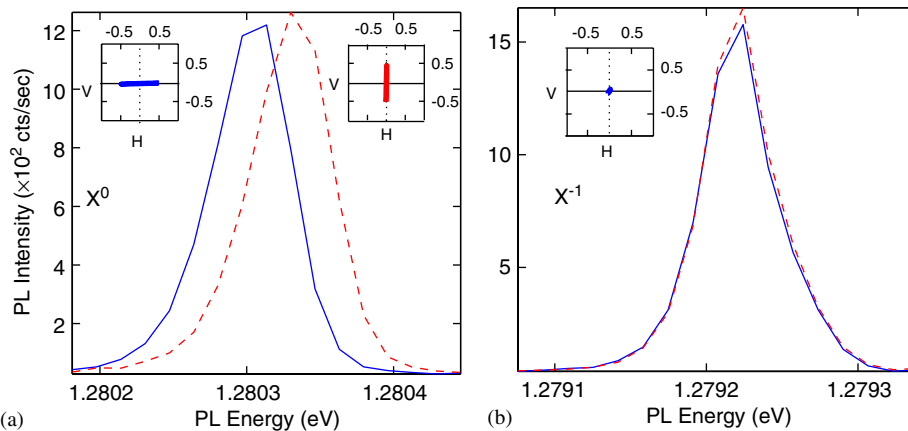


Fig. 1. Polarization sensitive PL spectrum of the (a) neutral and (b) charged excitons at zero magnetic field. The insets present the measured degree of polarization of the lines, where V (H) refers to the natural long (short) inplane axis of the QD.

excitation power (not shown [13]). The identification of these lines presents a challenge and it is not always straightforward. We used a set of complementary measurements for this task. PL as a function of intensity, is used to distinguish between single to multiple exciton lines [11,13], PL as a function of excitation energy (PLE) is used to distinguish between various charged state of the emitting QD [14] and intensity correlation measurements to confirm out assignments [12]. The presence of negatively charged emission lines is due to residual-ionized donor impurities in the vicinity of the QD. These donors contribute “resident” electrons to the QD. Neutral emission lines are observed when the electron from a photogenerated e–h pair deionize the donor and the unpaired hole recombine with the QD resident electron, thereby depleting the QD from its charge

[13]. As one reduces the excitation energy, the neutral lines lose strength and eventually vanish, since optical depletion is not possible with photon energy which is lower than that required to deionize the donor (not shown [13]). The polarization sensitive spectroscopy measurements which we present in Fig. 1 further confirms our line identifications. In Fig. 1, we present polarization sensitive high-resolution PL measurements of the neutral and the negatively charged excitons at zero magnetic field [13]. We accurately determined the polarizations of the observed lines from their Stokes coefficients by performing six different measurements with combinations of the orientation and retardation of the retarders. In the insets, the polarization state of the spectral lines in the plane of the sample is given relative to the natural axes of the QD. Fig. 1 demonstrates most clearly that while the neutral spectral line is composed of two cross linearly polarized doublets, the X^{-1} line has no fine structure and it is totally unpolarized. The anisotropic e–h exchange energy splitting for this QD as directly deduced by these measurements is $30\mu\text{eV}$. In Fig. 2, we present PL spectra of both the X^0 and X^{-1} lines at various magnetic fields. The figure demonstrates the diamagnetic shift of both spectral lines, their Zeeman splitting and the appearance of the “dark” excitonic transitions. The latter two are much more clearly presented in Fig. 3a (Fig. 3b) where the measured energies of the various optical transitions associated with the neutral (negatively charged) exciton are plotted as a function of the magnetic field, after subtraction of the diamagnetic shift. In Fig. 3, solid circles represent the measured energies, while solid lines represent our model calculations.

In Fig. 4, we present a comparison between the measurements to the results of the many body model calculations. The model assumes spherically symmetric lens

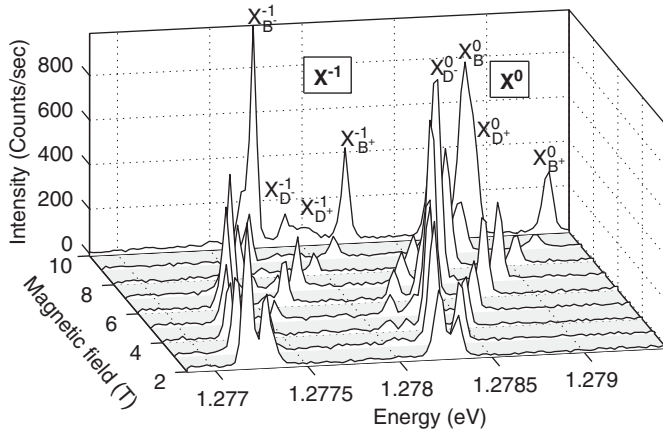


Fig. 2. PL emission spectra showing the single QDs X^0 and X^{-1} spectral lines at various applied magnetic fields in the Faraday configuration. The subscript B (D) denotes bright (dark) exciton.

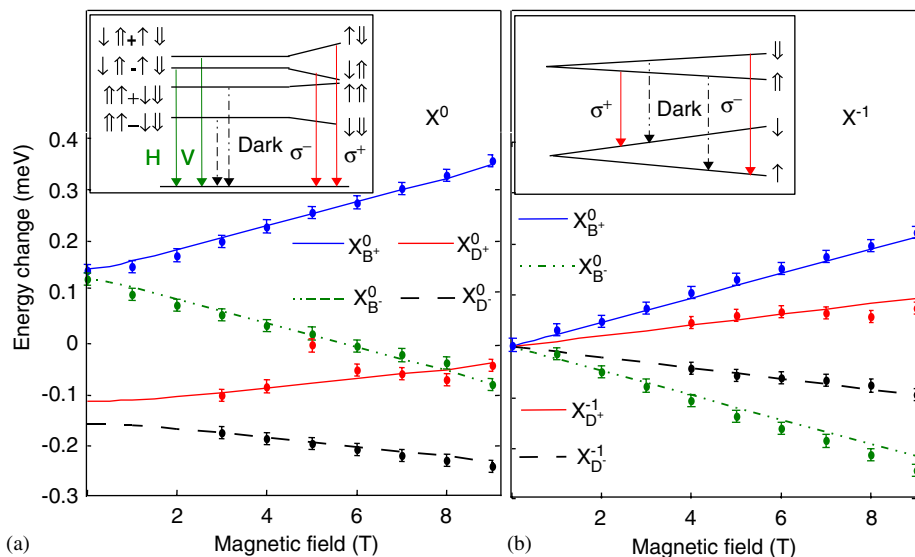


Fig. 3. Measured (symbols) and calculated (lines) energies of the PL lines associated with the (a) X^0 and (b) X^{-1} optical transitions (after subtracting the diamagnetic shift), as a function of the magnetic field strength. The insets describe the carriers’ spin wavefunctions associated with the various transitions.

Parameter	Experimental Value	Calculated Value	Units
X^0	1.2783 ± 0.0001	1.2760	eV
$X^0 - X^{-1}$	1.1 ± 0.2	0.7	meV
α^0	9.2 ± 0.2	9.7	$\mu\text{eV}/T^2$
α^1	8.8 ± 0.2	8.9	$\mu\text{eV}/T^2$
g_e	0.62 ± 0.05	—	—
g_h	0.26 ± 0.05	—	—
Δ_0	270 ± 30	—	μeV
Δ_1	30 ± 20	—	μeV
Δ_2	66 ± 20	—	μeV

Fig. 4. Comparison between measured and calculated QD magneto optical parameters. α^0 (α^1) is the diamagnetic shift coefficient for the X^0 (X^{-1}) line and g_e (g_h) is the electron (hole) inplane g -factor.

shape $\text{In}_{0.42}\text{Ga}_{0.58}\text{As}/\text{GaAs}$ QD with height of 11 monolayers and radius of 13.7 (12.7) nm for the electron (hole). The radii and the composition are the only fitting parameters in the model. The carriers effective masses and band offsets were calculated using an eight band $\mathbf{k} \cdot \mathbf{P}$ model [15], assuming pseudomorphic InGaAs strained layer. With these values, we solve one-band Schrödinger equations including the axial magnetic field for obtaining the single carriers' wavefunctions and energies. Then, a configuration interaction program is used to calculate the interactions between the carriers. We calculate e–e and h–h direct and exchange Coulomb interactions as well as the EHXI, for which we use the measured experimental parameters (Δ_0 , Δ_1 and Δ_2) for each e–h pair. As can be seen in Fig. 4, the agreement that we obtain with the measured data is quite remarkable. Our model describes well the absolute emission energies of both lines, the magnitude of the diamagnetic shifts of both lines and their evolution with the axially applied magnetic field. We note, however, that in order to obtain the measured intensity ratio between the bright and dark excitons, we had to assume photon propagation angle of 30° . This angle is much larger than the angle that we estimated from the detuning between the energy of the cavity mode and that of the spectral lines (7°). Misalignment between the QD symmetry axis and the magnetic field direction may contribute to this discrepancy [8].

In summary, we show experimentally and prove theoretically that planar microcavities allow simultaneous detection of both the bright and dark excitons in Faraday configuration. This phenomenon is used to measure the fine structure of the neutral and negatively charged single exciton states within the same single quantum dot. These measurements provide an accurate and most reliable determination of both the electron and hole g -factors (including their signs!) and their exchange–interaction parameters. Our measurements are in excellent agreement with many carrier model calculations which takes into account Coulomb and exchange interactions between all the present e–h pairs together with their interaction with a single cavity photon with propagation angle dictated by its detuning from the cavity-mode's energy.

Acknowledgments

The work was supported by the Israel Science Foundation, by the US–Israel Binational Science Foundation (BSF) and by the Technion Vice President Fund for the Promotion of Research at the Technion.

References

- [1] For a review see P. Michler, Topics Appl. Phys. 90 (2003) 315.
- [2] Z. Yuan, et al., Science 295 (2002) 102.
- [3] A. Zrenner, et al., Nature 418 (2002) 612.
- [4] C. Santori, et al., Nature 419 (2002) 594.
- [5] D. Loss, D.P. DiVincenzo, Phys. Rev. A 57 (1998) 120.
- [6] A. Imamoglu, et al., Phys. Rev. Lett. 83 (1999) 4204.
- [7] K.J. Vahala, Nature 424 (2003) 839.
- [8] M. Bayer, et al., Phys. Rev. B 65 (2002) 195315.
- [9] J.G. Tischler, et al., Phys. Rev. B 66 (2002) 813101.
- [10] E.L. Ivchenko, Optical Spectroscopy of Semiconductor Nanostructures, Alpha Science International Publishing, 2005.
- [11] E. Dekel, et al., Phys. Rev. Lett. 80 (1998) 4991.
- [12] D.V. Regelman, et al., Phys. Rev. Lett. 87 (2001) 257401.
- [13] N. Akopian, et al., in J. Menendez, C.G. Van de walle (Eds.), 27th International Conference on the Physics of Semiconductors Proceedings vol. 772, American Institute of Physics, 2005, p. 669.
- [14] D.V. Regelman, et al., Phys. Rev. B 64 (2001) 165301.
- [15] D. Gershoni, C.H. Henry, G.A. Baraff, IEEE J. Quantum Electron 29 (1993) 2433.